International Journal of Modern Manufacturing Technologies
ISSN 2067–3604, Vol. XVII, No. 3 / 2025
https://doi.org/ 10.54684/ijmmt.2025.17.3.108

MECHANICAL PROPERTIES OF 3D-PRINTED POLYLACTIDE CARBON FIBER BASED ON FUSED DEPOSITION MODELING

Mohamad Talhah Al Hafiz Mohd Khata[1], Nor Aiman Sukindar[1,2], Ahmad Shah Hizam Md Yasir[3], Shafie Kamaruddin[1], Muhamad Izzat Izzuddin Saharuddin[1], Ahmad Azlan Ab Aziz[4], Yang Chuan Choong[1], Wan Luqman Hakim Wan A Hamid[5], Muhammad Mukhtar Noor Awalludin[1]

[1]International Islamic University Malaysia, Manufacturing and Materials Department
Gombak, Selangor, Malaysia
[2]Universiti Teknologi Brunei, School of Design
Tunku Highway, Gadong BE 1410, Brunei Darussalam
[3]Rabdan Academy, Faculty of Resilience
65, Al Inshirah, Al Sa'adah, Abu Dhabi, 22041, PO Box: 114646, Abu Dhabi, UAE
[4]Universiti Teknologi Brunei, Engineering Faculty
Tunku Highway, Gadong BE 1410, Brunei Darussalam
[5]International Islamic University Malaysia, Department of Mechanical And Aerospace Engineering
Gombak, Selangor, Malaysia

Corresponding author: Nor Aiman Sukindar, noraimansukindar@gmail.com

Abstract: Three-dimensional (3D) printing, especially using fused deposition modeling (FDM), enables the creation of complex shapes while reducing material waste via a layer-by-layer deposition method. Determining the optimal printing parameters to improve the mechanical properties of printed components is a considerable problem. This study investigates the influence of printing factors, such as layer thickness, infill density, and printing speed, on the tensile and compressive properties of polylactic acid (PLA)-carbon fiber composites. A Taguchi orthogonal array design was utilized to examine nine experimental combinations of printing parameters and their impact on mechanical p. The results demonstrate that a layer thickness of 0.4 mm and an infill density of 80% yield a maximum tensile strength of 54.98 MPa. A layer thickness of 0.3 mm, an infill density of 80%, and a printing speed of 60 mm/s yield a compressive strength of 63.19 MPa. This study offers a thorough examination of parameter interactions and their effects, corroborated by scanning electron microscopy, setting it apart from previous research. The results offer substantial insights for optimizing the FDM process related to PLA-carbon fiber composites.
Keywords: Fused deposition modeling; three-dimensional printing; polyactide–carbon fiber; scanning electron microscopy; Taguchi method

1. INTRODUCTION

Fused Deposition Modeling (FDM), has attracted considerable interest for its capacity to produce intricate structures with minimal waste. Polylactic acid (PLA) has been a favored material in 3D printing owing to its biodegradability and diverse applications, including medical devices and packaging [1]. Nonetheless, the comparatively low mechanical strength of PLA restricts its employment in high-performance contexts, requiring investigations into reinforcement methods, especially the incorporation of carbon fibers, to improve its mechanical characteristics [2, 3]. Several printing parameters—including printing speed, infill density, and layer thickness—affect the mechanical characteristics of 3D-printed parts, including tensile and compressive strengths.

The three factors have been extensively studied because of their direct influence on the internal structure and interlayer adhesion of printed components [4, 5, 6]. The Taguchi approach was used in studies to evaluate how these factors affected the compressive strength of PLA-based scaffolds [4]. Similarly, another study [7] showed how important these factors were for the mechanical characteristics of 3D-printed carbon fiber–PLA composites. Other studies have looked at how changing these factors may improve the mechanical characteristics of PLA composites [8, 9, 10]. Using the Taguchi approach, a study methodically evaluated how printing speed, infill density, and layer thickness affected the tensile strength of carbon fiber-reinforced PLA

composites [8]. The study revealed that layer thickness significantly influenced tensile strength, while infill density also played a crucial role, while printing speed had a lesser impact. Our study extends this research by applying identical parameters to PLA-carbon fiber composites utilizing the Taguchi method, incorporating nine experimental variations. Specifically looking at the relationship between tensile and compressive strengths in carbon fiber-reinforced PLA, we expand our study to cover both. Particularly stressing the interaction between tensile and compressive strengths, an area that has been under-researched in other studies, this approach offers deep insights into the combined influence of several factors.

Apart from these main 3D printing parameters, extrusion temperature, nozzle size, and printing patterns are other elements that greatly affect the mechanical characteristics of produced components.

For instance, extrusion temperature directly affects the bonding between printed layers, with optimal temperatures improving layer adhesion and mechanical strength [11]. Similarly, nozzle diameter impacts precision and material deposition, where smaller nozzles can produce finer details but larger nozzles enable faster printing, potentially sacrificing resolution [12]. Printing patterns affect internal structure and force distribution, as differing infill orientations yield different tensile and compressive strengths [13]. Despite the comprehensive research, the combined impact of printing speed, infill density, and layer thickness on the tensile and compressive strengths of PLA-carbon fiber composites remains inadequately investigated. While previous research has examined these characteristics either in isolation or within disparate contexts [14, 15], there is a gap in the literature regarding their systematic evaluation for composite materials. Additionally, although there are existing studies on the optimization of these parameters, many have not specifically addressed the interplay of these factors in PLA-carbon fiber composites, which are known to exhibit complex mechanical behaviors due to their anisotropic nature [16, 17, 18].

Using the Taguchi approach to systematically investigate the effects of printing speed, infill density, and layer thickness on the tensile and compressive strengths of PLA-carbon fiber composites, we seek to fill this gap in this work. A design of experiments approach was used to test nine different combinations of these variables in order to find the optimal values improving the tensile and compressive strength of the composite material. This study aims to help 3D printing procedures for PLA-carbon fiber composites by emphasizing these important elements, hence setting itself apart from earlier studies that have either investigated fewer variables or other materials [19].

2. MATERIALS AND METHODS

2.1. Material

A polylactic acid filament with a carbon-fiber composite has been used in this study. The filament measures 1.75 mm and is sourced from SUNLU (Sunlu, Zhuhai). The manufacturer's specifications indicate that the filament comprises 70%–80% polylactide resin, 10%–20% carbon fiber, and 10% additives. The manufacturer advises utilizing a hardened steel nozzle with a diameter of 0.6 mm or larger, given the abrasive characteristics of carbon fiber, to avoid clogging and minimize wear. Although smaller nozzles (e.g., 0.4 mm) are commonly used for pure PLA, the composite material requires a larger nozzle to accommodate fiber particles and avoid damage.

Based on this recommendation, a 0.8-mm hardened steel nozzle was used in this study, offering several key advantages. The larger diameter reduces the risk of clogging, ensures smooth extrusion, and minimizes mechanical wear, making it more suitable for carbon-fiber composites large nozzle also helps to create thick extrusion layers, consequently improving layer adhesion, which is especially important for optimizing the mechanical properties of the composite. A different study [20] on carbon-fiber-reinforced PLA composites underlined the effect of nozzle diameter on mechanical parameters, including tensile strength and fatigue life.

Their findings show that a large nozzle diameter enhances the strength and print consistency, particularly for abrasive materials like carbon-fiber composites. This supports the use of a 0.8-mm nozzle as it minimizes clogging and improves the extrusion quality, leading to better overall mechanical properties. Table 1 shows the filament specifications.

2.2. Method

Before the experiment, the printing parameters (speed, infill density, and layer thickness) were determined. The manufacturer recommended a bed temperature of 60°C to 80°C and a printing temperature of 200°C to 230°C. Based on our initial printing test using our 3D printer, a nozzle temperature of 200°C and a bed temperature of 80°C were chosen because they produce consistent results and exhibit less failure. While the extrusion temperature was set to 200°C, variations in the extrusion temperature could considerably affect the material viscosity, as highlighted by [21], which could in turn influence the layer bonding and tensile strength of the

composite. While high extrusion temperatures might improve the interlayer adhesion, they could cause issues such as warping if not controlled properly. By orienting rasters in the direction of the applied force, the raster angle was set at 0°, hence producing ideal tensile results. Still, [22] found that usually increasing anisotropy with a raster angle of 0° made the material more prone to breaking under multidirectional pressures. Alternative raster angles, such as +45°/−45°, could improve isotropy and better distribute mechanical forces across multiple directions. Thus, raster angle selection should be based on the intended application of printed components to find a balance between strength and flexibility. The layer thickness used was 0.2, 0.3, or 0.4 mm, printing speed of 30, 60, or 90 mm/s was used, and the infill density was set to 20%, 50%, or 80%. The values of these parameters were determined based on the midpoint of each printing parameter, which is the default setting of the 3D printer. The printer was an Artillery Sidewinder X1 3D printer (Shenzhen, China), and its control parameters are listed in Table 2.

Table 1. Physical properties of the filament according to manufacturer.

Properties	Value
Print temperature (C°)	200–230
Bed temperature (C°)	60
Density (g/cm)	90
Heat distortion temperature (C°, 0.45 MPa)	30
Melt flow index (g/10 min)	60
Tensile strength (MPa)	90
Elongation at break (%)	30
Flexural strength (MPa)	60
Flexural modulus (MPa)	90
Izod impact strength (kj/m)	4

Table 2.Printing parameters recommended by the manufacturer.

Properties	Value
Nozzle diameter (mm)	0.8
Printing temperature (C°)	200
Raster angle (°)	0.0
Bed temperature (C°)	80
Infill density (%)	20, 50, and 80
Infill pattern	Cubic
Layer height (mm)	0.2, 0.3, and 0.4
Wall count	2
Top layer	4
Bottom layer	4
Nozzle diameter (mm)	0.8

2.3. Sample Preparation

Mechanical tests were conducted on a universal testing machine. The tensile and compressive strength tests adhered to ASTM standards D638 Type-IV and D695, respectively. The ASTM D638 Type-IV standard mandates that tensile tests be conducted on dog-bone shaped specimens, which are optimal for evaluating very soft polymers and for comparing materials of varying stiffness. The specimens must possess a gage length of 25 mm, a narrow parallel section width of 6 mm, shoulders measuring 19 mm in width, and an overall length of 115 mm.. The thickness is material-dependent but typically falls within the 3–14 mm range. Specimens of thickness 3 mm were prepared for the present study. This specific geometry properly balances the gripping

strength against stress concentration along the gage length, allowing accurate tensile testing of soft materials. The developed design is illustrated in Figure 1.

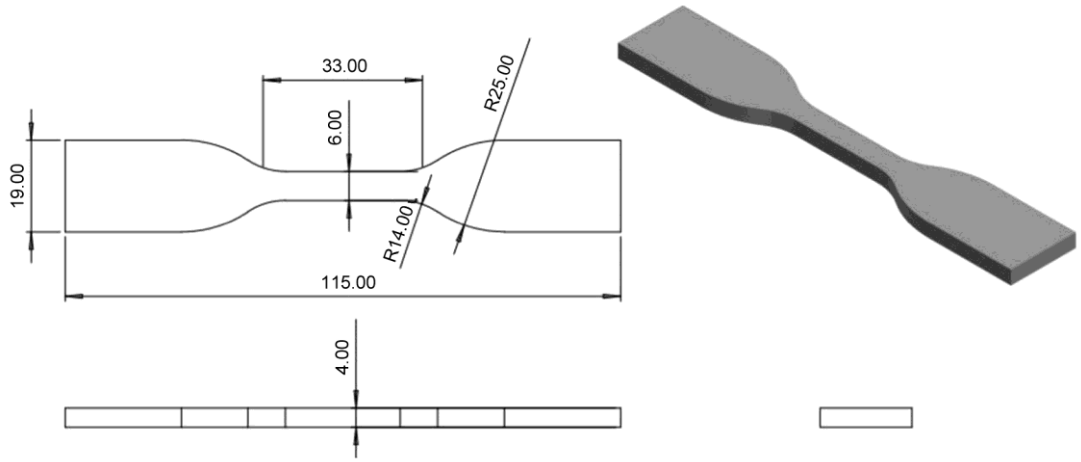

Fig 1. Isometric view of a specimen designed for tensile tests according to the ASTM D638 Type-IV standard using SolidWorks 2022

Compressive tests were performed on cylindrical specimens. A specimen of the common dimensions (diameter = 12.7 mm; length = 25.4 mm) is compact and ideally suited for measuring various compressive properties such as ultimate strength and modulus. The design is shown in Figure 2. To establish an effective table for measuring the variations among the samples, this study implements the Taguchi technique using Minitab 21.0 (Minitab, USA) software. Table 2 shows the printing parameters selected for tensile and compressive tests of the PLA–carbon fiber. The Minitab package allows use of the Taguchi method, which allows systematic optimization of product or process performance, reduces variability, and improves quality while also considering the cost factors.

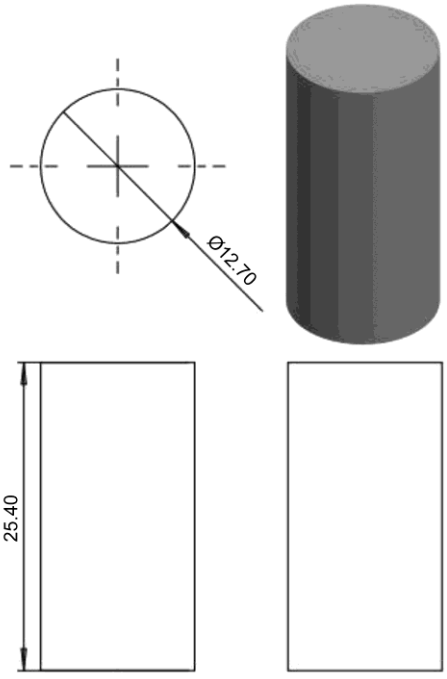

Fig 2. Isometric view of the cylindrical specimens designed for compressive tests according to the ASTM D695-15 standard using SolidWorks 2022

The efficient design of experiments, statistical analysis, and robustness focus of the Taguchi method improve the outcomes and increase the efficiency of engineering and manufacturing processes. In this study, nine runs of experiments (three levels each of the layer thickness, printing speed, and infill density) were designed for the tensile tests. Further, another nine runs of experiments were designed for the compressive tests. Each run of the experiment was repeated 5 times to ensure data consistency and reliability; hence, from 9 runs each of tensile and compressive strength experiments, 90 samples were produced and tested in total during this study.

3. RESULTS

3.1. Experimental results of tensile strength

A total of nine runs of the experiment were performed for the tensile strength test. Each run of the experiment was repeated 5 times to ensure data reliability and consistency. Forty-five samples of PLA–carbon fiber were 3D-printed using the FDM process. The tensile strength data were analyzed using the Taguchi method, and tensile tests were conducted on a universal tensile machine (SHIMADZU AGS-5KNX, Kyoto, Japan) under controlled laboratory conditions. The testing speed was set to 10 mm/min as per the ASTM D638 Type-IV standards. The tests were performed at room temperature (23°C) and 50% relative humidity to ensure consistency across all trials. These environmental conditions were maintained to minimize any variation in the mechanical properties that could be attributed to external factors such as temperature or humidity. For tensile tests, strain was measured experimentally using an extensometer attached to the specimen during testing with a SHIMADZU AGS-5KNX machine. This ensured precise deformation tracking. The tensile strain data were recorded directly from the displacement of the extensometer, which enabled highly accurate strain measurement. A sample with higher tensile strength is resistant to breakage under tension, indicating superior strength and durability. Conversely, a sample with lower tensile strength is easily deformed. Table 3 displays the experimental results of the samples with different printing parameters. The tensile strength of each sample was measured 5 times (n = 5), and the results were averaged to obtain a precise final result.

Table 3. Results of tensile test

Run	Layer Thickness (mm)	Printing Speed (mm/s)	Infill Density (%)	Average Tensile Strength (MPa)
1	0.2	30	20	41.65
2	0.2	60	50	42.83
3	0.2	90	80	48.84
4	0.3	30	50	43.71
5	0.3	60	80	46.18
6	0.3	90	20	43.16
7	0.4	30	80	54.98
8	0.4	60	20	48.14
9	0.4	90	50	51.22

Table 3 indicates that a layer thickness of 0.4 mm, an infill density of 80%, and a printing speed of 30 mm/s (experimental run 7) maximized the tensile strength at 54.98 MPa. The second and third best designs were experimental runs 9 and 3, with average tensile strengths of 51.22 MPa and 48.84 MPa, respectively. By comparison, experimental run 1, defined by a layer thickness of 0.2 mm, an infill density of 20%, and a printing speed of 30 mm/s, produced the lowest tensile strength at 41.65 MPa. While Figure 3b shows those for Run 7, showing the lowest and highest tensile strength values, respectively, Figure 3a shows the tensile stress–strain curves for Run 1. Sample 1's condition following the tensile test is seen in Figure 4.

The tensile stress-strain curves showing the mechanical characteristics of two samples—Run 1, showing the lowest tensile strength, and Run 7, showing the highest tensile strength—are shown in Figures 3a and 3b. As illustrated in Figure 3a, Run 1, printed at a lower infill density (20%), exhibited a strain-to-break of 26%, even though its tensile strength was relatively low at 41.65 MPa. The higher strain-to-failure suggests that, despite its lower tensile strength, Run 1 retained more flexibility and deformed significantly before failure. This behavior is likely due to the less rigid internal structure, which allowed for greater elongation under tensile load before

fracturing. By contrast, Figure 3b shows that Run 7, printed at 80% infill density, exhibited a much higher tensile strength of 54.98 MPa but had a lower strain of approximately 8%.

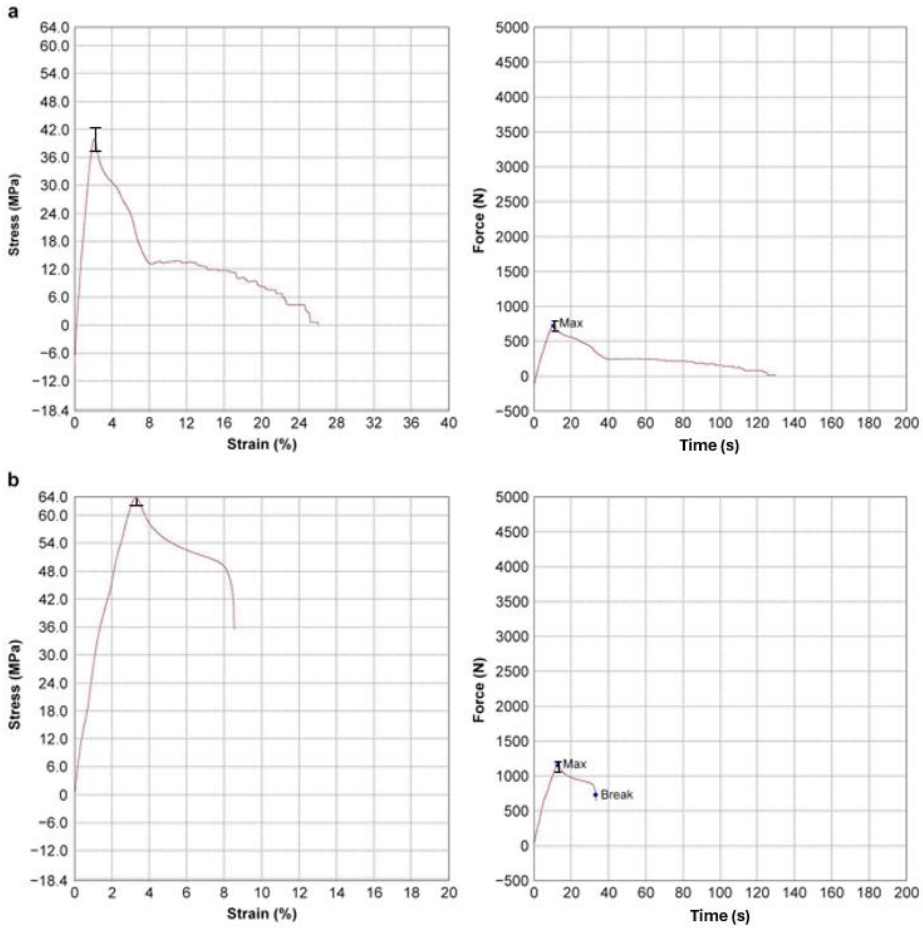

Fig 3 . Tensile stress–strain curves of a) experimental run 1 and b) experimental run 7

Fig 4 . Sample Run 1 after the tensile test (layer thickness = 0.2 mm, printing speed = 30 mm/s, infill density = 20%)

The reduced strain-to-failure indicates that the brittleness of the material increased with the tensile strength. The denser internal structure, while improving strength, reduced the composite's ability to deform under load, leading to fracture occurrence earlier than that observed in Run 1. These results were consistent with literature. Studies have shown that carbon-fiber-reinforced PLA composites exhibited increased strength with increasing infill densities but tended to break more suddenly under tensile stress [23]. Similarly, the addition of chopped carbon fibers improved tensile strength but might reduce ductility, resulting in lower strain-to-failure [24]. The

higher strain observed at break in Run 1 (26%) than in Run 7 (8%) could be attributed to internal voids in Run 1, which allowed for more elongation before failure, while the denser structure in Run 7 limited deformation. Thus, an increased infill density reduces voids and enhances material rigidity, which can improve strength but reduce flexibility [25].

3.2. Experimental results of compressive strength

This subsection applies the Taguchi method to the compressive strength data of 45 PLA–carbon-fiber samples 3D-printed using the FDM processFollowing ASTM D695 standards, universal tensile machines(SHIMADZU AGS-5KNX and SHIMADZU UH-X/FX Series) were used to conduct compressive testing at a constant speed of 10 mm/min. To offer consistent testing conditions, the studies were carried out under same environmental conditions—room temperature of 23°C and 50% relative humidity. Additionally, SHIMADZU AGS-5KNX was used for analyzing specimens expected to withstand loads below 60 MPa, while UH-X/FX Series was employed for higher load-bearing specimens, which provides accurate results for samples requiring forces up to 100 MPa. Samples 1, 2, 6, and 8 were tested on the AGS-5KNX model, which cannot exert more than 60 MPa whereas samples 3, 4, 5, 7, and 9 were tested on the UH-X/FX Series, which exerts a maximum force of 100 MPa. For compression tests, strain was determined by the displacement of the compression plates on the SHIMADZU UH-X/FX Series machine. The machine calculated the strain based on changes in the specimen length during the application of compressive force. In compressive tests, samples with higher compressive strength, such as Run 5 (63.19 MPa), demonstrated superior load-bearing capacity with minimal deformation. This finding was consistent with [16], which reported that higher infill densities in PLA composites lead to a denser internal structure, improving the load distribution and compressive strength. The microstructural analysis shown in Figure 15 confirms this observation as samples with higher infill density showed fewer internal voids, leading to enhanced structural integrity. Table 4 presents the experimental outcomes of the samples produced under various printing conditions. The compressive strength of each sample was assessed five times. (n = 5) and the results were averaged to provide a precise final result.

Table 4 . Results of test

Run	Layer Thickness (mm)	Printing Speed (mm/s)	Infill Density (%)	Average Strength (MPa)
1	0.2	30	20	37.82
2	0.2	60	50	35.35
3	0.2	90	80	51.63
4	0.3	30	50	49.11
5	0.3	60	80	63.19
6	0.3	90	20	38.80
7	0.4	30	80	61.08
8	0.4	60	20	36.57
9	0.4	90	50	47.56

In Table 4, Experimental Run 5, defined by a layer thickness of 0.3 mm, an infill density of 80%, and a printing speed of 60 mm/s, indicates the compressive strength reaching its peak at 63.19 MPa. With average compressive strengths of 61.08 MPa and 51.63 MPa, respectively, experimental Runs 7 and 3 were the second and third top performers. However, experimental Run 2, defined by a layer thickness of 0.2 mm, an infill density of 50%, and a printing speed of 60 mm/s, had the lowest compressive strength at 35.35 MPa. While Figure 6 shows the state of the sample from experimental Run 2 after compressive testing, Figure 5 shows the compressive stress-strain curves from the experiment for the least compressive value (Run 2).

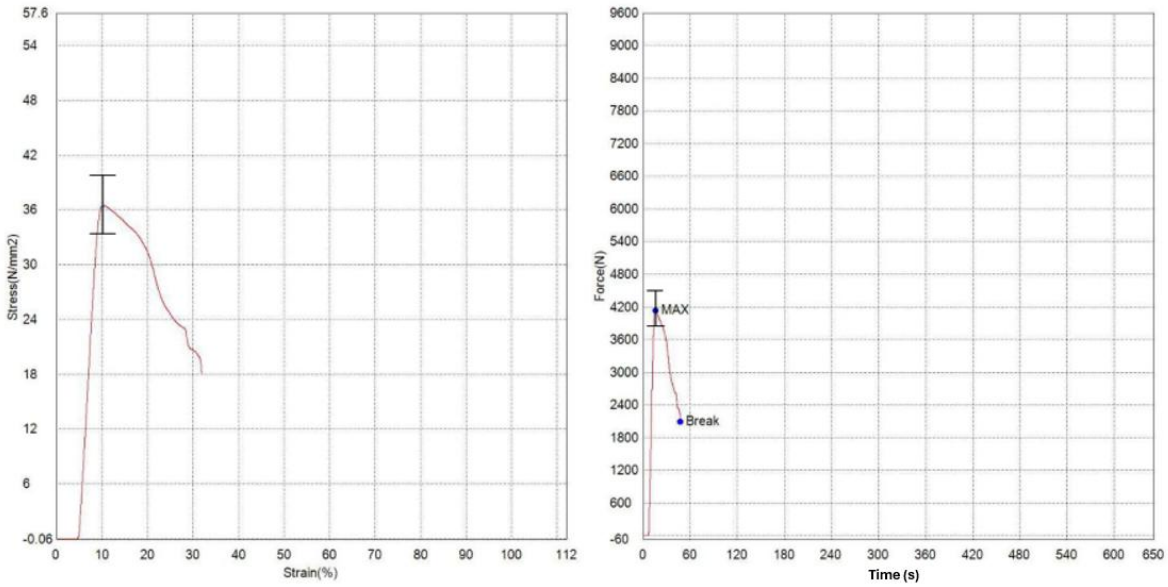

Fig 5 . Compressive stress–strain curves of experimental run 2

Fig 6 . Sample 2 after the compressive test (layer thickness = 0.2 mm, printing speed = 30 mm/s, and infill density = 20%)

4. RESULTS AND DISCUSSION

4.1. Analysis of variance of tensile strength

The means among the experimental groups were compared using the Analysis of Variance (ANOVA) technique. The ANOVA results are listed in Table 5.

Table 5. Results of the ANOVA tests on tensile strength

Source	DF[a]	Adj SS[b]	Adj MS[c]	F-Value
Layer Thickness	2	99.464	49.7321	138.69
Printing Speed	2	6.146	3.0731	8.57
Infill Density	2	51.517	25.7587	71.84
Error	2	0.717	0.3586	
Total	8	157.845		

[a]Degrees of freedom; [b][Adjusted sum of squares]; [c][Adjusted mean squares]

The ANOVA test at the 0.05 significance level indicated that layer thickness ($p = 0.007$) significantly affects the response variable ($p < 0.05$); thus, the observed variations in tensile strength due to differing layer thickness are unlikely to be attributed to chance and can be ascribed to layer thicknessThe adhesion between the materials increases with higher layer thickness. The infill density significantly affects the tensile strength of the printed samples ($p = 0.014$). The tensile strength is not substantially affected by printing speed ($p = 0.104$). Figure 7 demonstrates that the average tensile strength remained stable as the layer thickness grew from 0.2 to 0.3 mm, but saw a significant increase with a further increase to 0.4 mm.

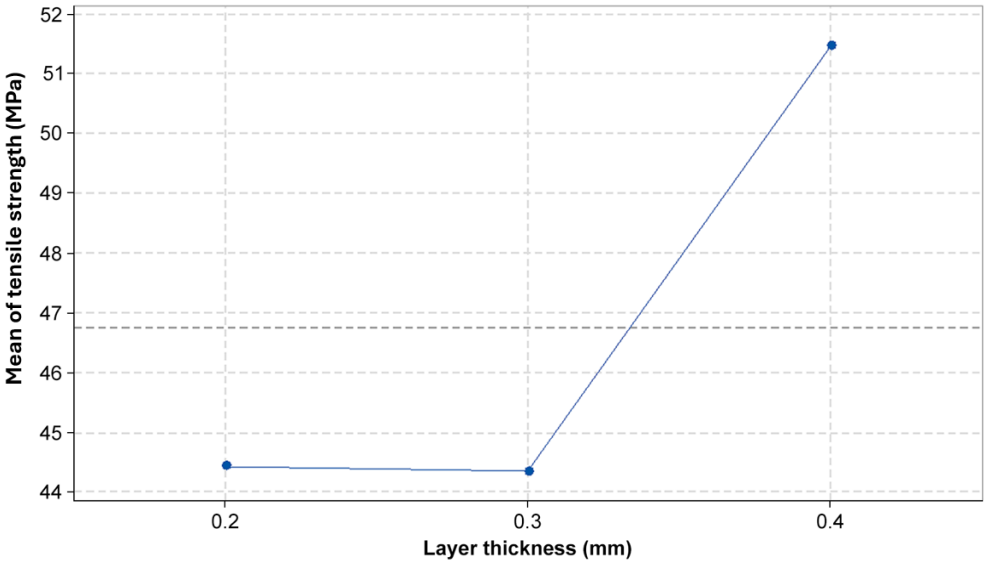

Fig. 7. Main effect plots of the layer thickness

4.1.1. S/N ratios and means

Table 6 is a response table illustrating the means of the three variables. The layer thickness is the most significant factor (delta = 7.10), followed by infill density and printing speed. The effects of various parameters on tensile strength responses are illustrated as main effect plots in Figure 8. In a main effect plot, points approximating a horizontal line signify a comparatively low significance level of the variable on the analyzed effect, whereas points presenting the steepest slope signify the most substantial impact of the variable on the response. The slope is indicated as the mean inclination with respect to the *x*-axis. The data in Figure 8 suggest that layer thickness considerably influences the tensile strength.

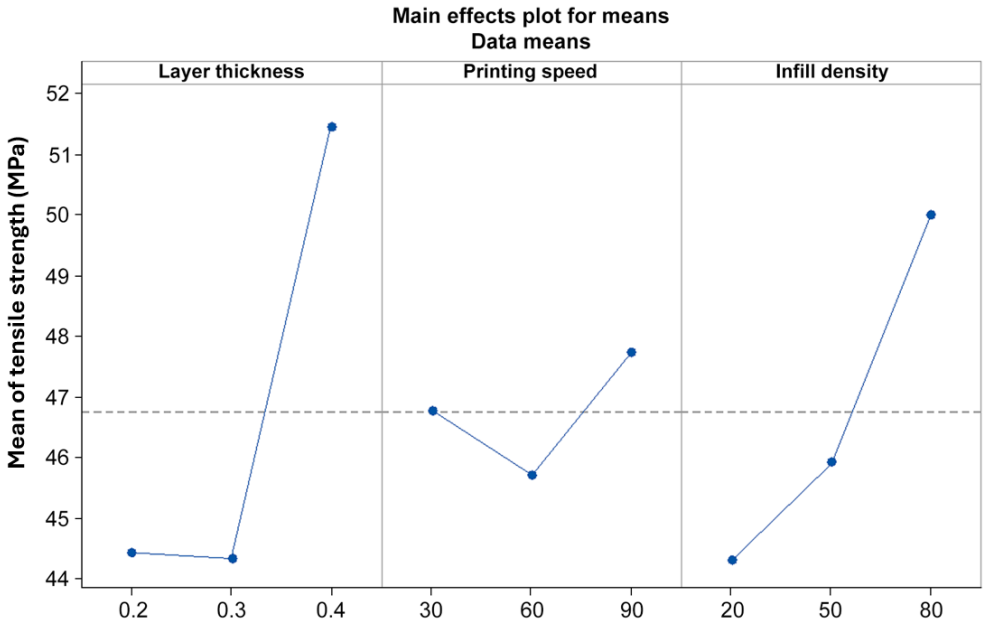

Fig. 8. Main effect plots of mean tensile strengths

Table 6. Response table of means of tensile strength

Level	Layer Thickness (mm)	Printing Speed (mm/s)	Infill Density (%)
1	44.44	46.78	44.32
2	44.35	45.72	45.92
3	51.45	47.74	50.00
Delta	7.10	2.02	5.68
Rank	1	3	2

Table 7 is the response table of the signal-to-noise ratios, which provides a reference for selecting the optimal value of each factor. The parameter that most significantly influences the tensile strength was determined from the delta values, which are ranked from highest to lowest. According to the S/N ratios presented in Table 7, layer thickness is the most influential parameter of surface roughness. The first-ranked parameter was layer thickness, with a delta value of 1.28, followed by infill density and finally by printing speed.

Table 7. Response table of signal-to-noise ratios for tensile strength

Level	Layer Thickness (mm)	Printing Speed (mm/s)	Infill Density (%)
1	32.93	33.34	32.91
2	32.93	33.19	33.21
3	34.21	33.56	33.96
Delta	1.28	0.36	1.04
Rank	1	3	2

The tensile strength response was optimized using a "larger-is-better" objective function [8] to determine the values of the process parameters and enhance tensile strength. An improved signal-to-noise ratio correlates with superior mechanical properties [26]. The major effect plots in Figure 9 demonstrate that an increased S/N ratio correlates with greater tensile strength. Table 8 establishes the values and levels of the process parameters that maximize tensile strength, as deduced from the main effect plots of S/N ratios.

.

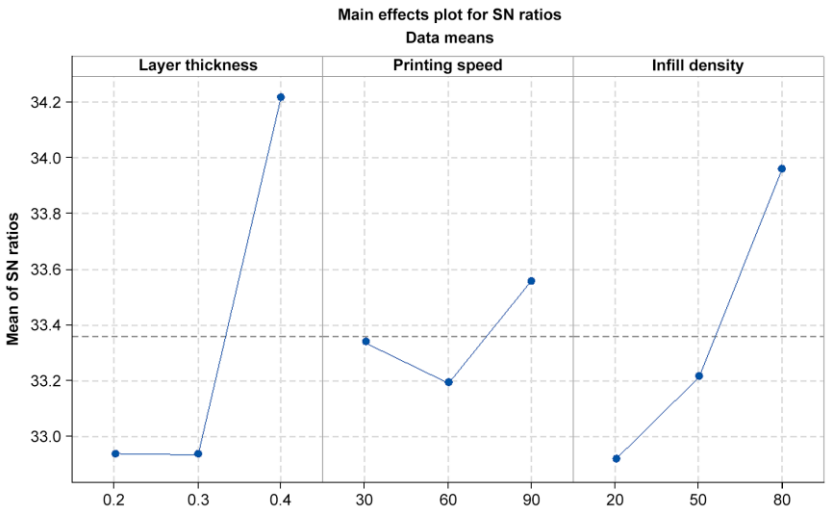

Fig 9 . Main effect plots of S/N ratios for tensile strength

Table 8. Optimum parameter settings for the tensile test

Layer thickness (mm)	Printing speed (mm/s)	Infill density (%)	Layer thickness (mm)
0.4	90	80	0.4

Supposedly, the tensile strength can be enhanced by increasing the layer thickness and infill density and lowering the printing speed [2]. Augmented infill densities typically raise the tensile strength by compacting the internal structure and adding reinforcement [3]. Elevated printing speeds can potentially bolster productivity but compromise the tensile strength. Contrary to these expectations, printing speed was positively correlated with tensile strength in the present study. The speed and quality must be delicately balanced to avert detrimental impacts on the material properties. Slower printing speeds often improve the precision of material deposition, the bonding properties, and fiber alignment to enhance the tensile strength. By systematically adjusting these parameters and assessing the resulting tensile strength, one can identify the ideal combination of layer thickness, infill density, and printing speed for PLA-carbon-fiber 3D printing, potentially producing high-quality, durable components with enhanced tensile strength that fulfill the requirements of their intended applications.

4.1.2. Analysis of printing parameters

Using the Taguchi statistical method, the process parameters were adjusted to maximize tensile strength by thoroughly examining the correlations and interactions among layer thickness, infill density, and printing speed. Layer thickness's effect on the tensile strength of PLA-carbon fiber mirrors the principles of traditional 3D printing methods. Thinner layers in PLA–carbon-fiber printing enhance tensile strength by increasing interlayer bonding [10]. The strong adhesion between the carbon-fiber-infused PLA layers leads to a homogeneous structure that potentially raises the tensile strength [1]. Conversely, thicker layers might introduce porosity and weak points that diminish the overall tensile strength. Moreover, as the carbon fibers are aligned, PLA–carbon-fiber composites are inherently anisotropic, and their bonding behavior and layer orientation determine their mechanical properties [2]. The tensile strength increased as the layer thickness grew; specimens with 0.2 mm, 0.3 mm, and 0.4 mm layers had tensile strengths of 48.84 MPa, 46.18 MPa, and 54.98 MPa, respectively, which goes against conventional understanding and previous research. The sample produced with 0.4mm thick layers exhibited a notably higher tensile strength than the samples produced with thinner layers. This unexpected result could be linked to the distinctive characteristics of the PLA–carbon-fiber composite material. Increasing the layer thickness likely promoted the alignment and distribution of carbon fiber inside the layers, hence raising load-bearing capacity and overall strength [18]. Increasing the layer thickness concurrently diminishes the quantity of interfaces, potentially reducing the number of weak points or discontinuities within the structure, hence enhancing tensile strength.. Figure 10 compares the microstructures of sample 5 (Figure 10a) and sample 7 (Figure 10b) at layer thicknesses of 0.3 and 0.4 mm, respectively. Clearly, the carbon fibers more effectively improve the tensile strength in thicker layered samples than in thinner layered samples. Carbon fibers, known for their high strength and stiffness, provide reinforcement when embedded in a PLA matrix. The strong and rigid carbon fibers enhance the deformation resistance and overall strength of the material.

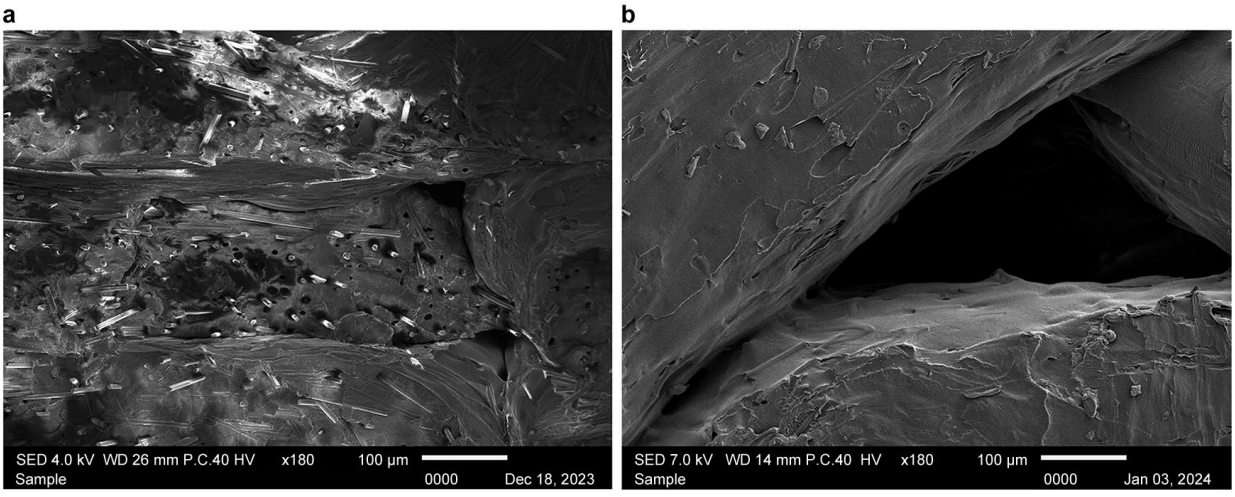

Fig. 10. Comparison of microstructures of a) sample 7 with a layer thickness of 0.4 mm and b) sample 5 with a layer thickness of 0.3 mm (scale bar = 100 µm) in the tensile strength experiment.

Tensile strength is usually positively correlated with infill density. For instance, the data of Table 3 show a tensile strength increase of 41.65 to 54.98 MPa as the infill density rises from 20% to 80%. This enhancement can be attributed to the resilient, minimally porous structure with elevated infill density, capable of enduring high tensile stress [27]. The observed positive correlation between tensile strength and infill percentage can be ascribed to the increased density and diminished number of air voids, both of which mitigate the possibility for deformation.. The microstructures of the samples with infill densities of 20% and 80% show marked differences (Figure 11a); in particular, the number of voids or gaps within the printed component is increased at the 20% infill density. The voids appear between the printed layers and within the infill structure, potentially serving as stress concentrators and vulnerable points that tend to fail under an applied load. Moreover, decreased material filling could compromise interlayer adhesion, weakening interlayer bonding and consequently reducing the overall structural integrity of the printed component [16]. These circumstances have the potential to diminish the printed part's mechanical properties, which in turn lowers its overall performance when contrasted with components made with higher infill densities.

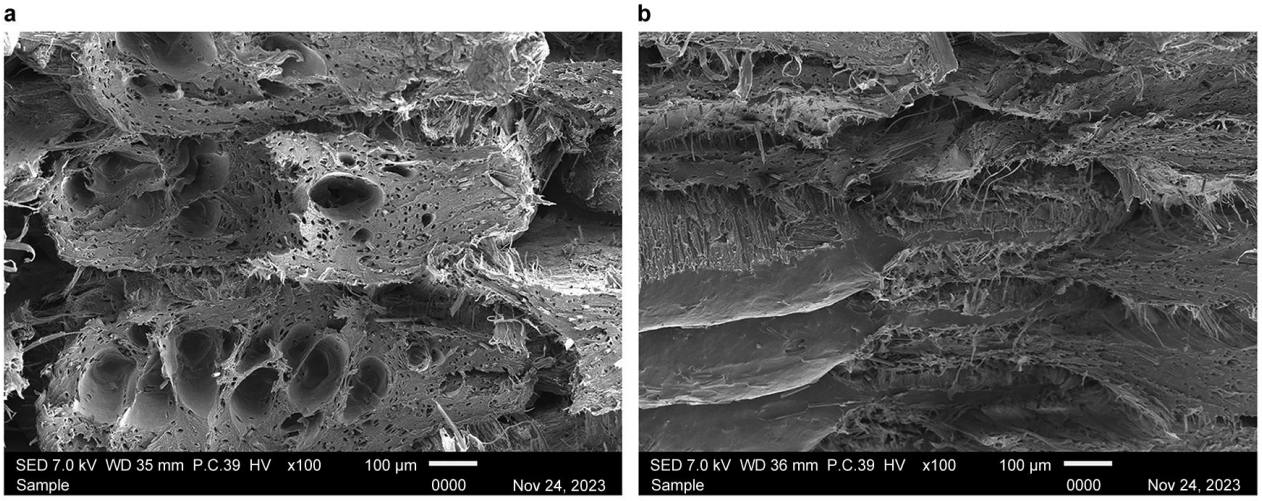

Fig 11. Microstructural comparison of samples with infill densities of a) 20% and b) 80% (scale bar = 100 µm) in tensile strength experiment.

At an infill density of 80% (Figure 11b), the structure is densely compact with a high degree of carbon-fiber reinforcement and minimal spacing between adjacent lines. The amplified density enhances the resistance of this specimen to applied loads, so the strength is maximized at this infill rate. The high material volume per layer and improved interlayer bonding diminish the number of voids, creating a robust and continuous microstructure. Moreover, the tight gaps between neighboring layers minimize the airflow, reducing the heat convection and elevating the crystallinity of the structure [16]. In summary, the dense microstructure offers superior support and minimizes the risk of warping or distortion during the printing process. Hence, it was inferred that high infill density boosts the quantity of carbon-fiber reinforcement within the printed sample, thereby enhancing its load-bearing capability and resilience against tensile forces.

As indicated in Table 5, printing speed exerted no consistent impact on tensile strength. The highest average tensile strength (54.98 MPa) was shown by sample 7, which had a layer thickness of 0.4 mm, an infill density of 80%, and a printing speed of 30 mm/s. Samples 9 and 8 were next, printing at 90 mm/s and 60 mm/s, respectively, with average tensile strengths of 51.22 and 48.14 MPa. Clearly, the tensile strength was neither positively nor negatively related to printing speed. High printing speed might improve the interlayer bonding by increasing the melt fusion between adjacent layers. The fast deposition and melting of material promote strong bonding, forming a solid, cohesive microstructure. Furthermore, elevated printing speeds create dense material deposits, minimizing the presence of voids, hence enhancing structural integrity and augmenting the total tensile strength of the printed item. The tensile mechanical properties of continuous carbon-fiber-reinforced composites are considerably influenced by relative fiber content rather than by printing temperature and speed [4]. This is primarily because the fiber content affects the fiber-matrix bonding surfaces in the composites [17], as the continuous carbon fibers create a reinforcing phase that impacts the tensile mechanical properties of the composite. The findings indicate that the printing speed does not have a significant impact on the tensile strength of PLA–carbon fiber.

4.2. ANOVA for compressive strength

The compressive strengths of the samples were analyzed through an ANOVA analysis at the 0.05 significance level, as described for the tensile strengths. The results are listed in Table 9.

Table 9. Results of the ANOVA tests on compressive strength

Source	DF[a]	Adj SS[b]	Adj MS[c]	F-Value
Layer Thickness	2	126.99	63.50	3.70
Printing Speed	2	30.57	15.28	0.89
Infill Density	2	690.29	345.14	20.10
Error	2	34.34	17.17	
Total	8	882.19		

[a]Degrees of freedom; [b][Adjusted sum of squares]; [c][Adjusted mean squares]

As shown in Table 9, the infill density ($p = 0.047$) significantly affects the response variable (p-value < 0.05), indicating that the observed differences in compressive strength are truly attributable to the variations in infill density. This result indicates enhancement of the bonding between the materials. The compressive strength of the specimen (Figure 12) rose as the infill density went up from 20% to 80%. The ANOVA results showed no significant impact on the compressive strength of the printed samples from layer thickness ($p = 0.213$) or printing speed ($p = 0.673$).

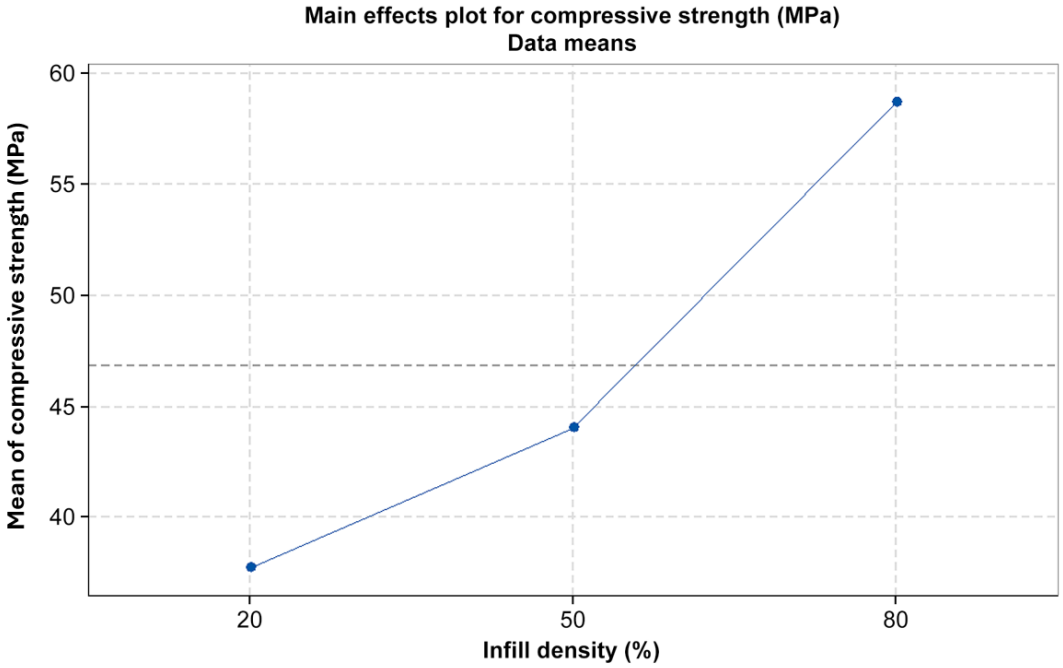

Fig. 12. Main effect plot of compressive strength against infill density

Similar to the tensile test, a response table of signal-to-noise ratios (Table 10) was constructed as a reference for selecting the optimal level of each factor. The primary parameter influencing compressive strength was determined from the delta and rank values. The S/N ratios in Table 10 indicate that infill density had the most substantial impact on compressive strength. The infill density received a ranking of 1, with an associated delta value of 3.80. The characteristics ranked second and third were layer thickness and printing speed, respectively. Table 11 is a response table of the means for compressive strength. The infill density ranks highest (delta = 20.90), succeeded by layer thickness and printing speed. Figure 13 presents the primary effect plots demonstrating the influence of process parameters on compressive strength. The plot indicates that infill density has a greater impact on compressive strength than layer thickness and printing speed.

Table 10 . Response table of signal-to-noise ratios for compressive strength

Level	Layer Thickness (mm)	Printing Speed (mm/s)	Infill Density (%)
1	32.26	33.70	31.53
2	33.87	32.75	32.78
3	33.51	33.19	35.33
Delta	1.61	0.95	3.80
Rank	2	3	1

Table 11. Response table of means for compressive strength

Level	Layer Thickness (mm)	Printing Speed (mm/s)	Infill Density (%)
1	41.60	49.34	37.73
2	50.37	45.04	44.01
3	48.40	46.00	58.63
Delta	8.77	4.30	20.90
Rank	2	3	1

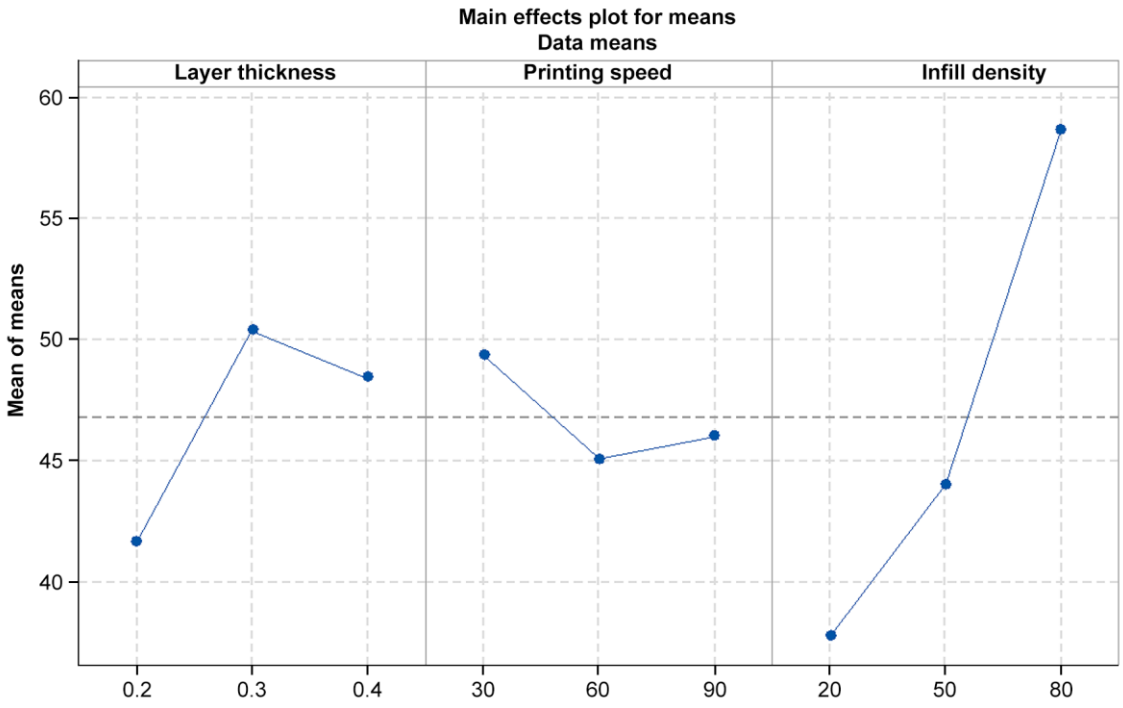

Fig. 13. Main effect plots of means of compressive strength

Likewise to the tensile strength response, the compressive strength response was optimized using a "larger-is-better" objective function to ascertain the optimal levels of the process parameters. The primary effect graphs (Figure 14) illustrate that an elevated S/N ratio correlates with increased compressive strength. The ideal process parameter values and their corresponding levels derived from the linear graphs are presented in Table 12.

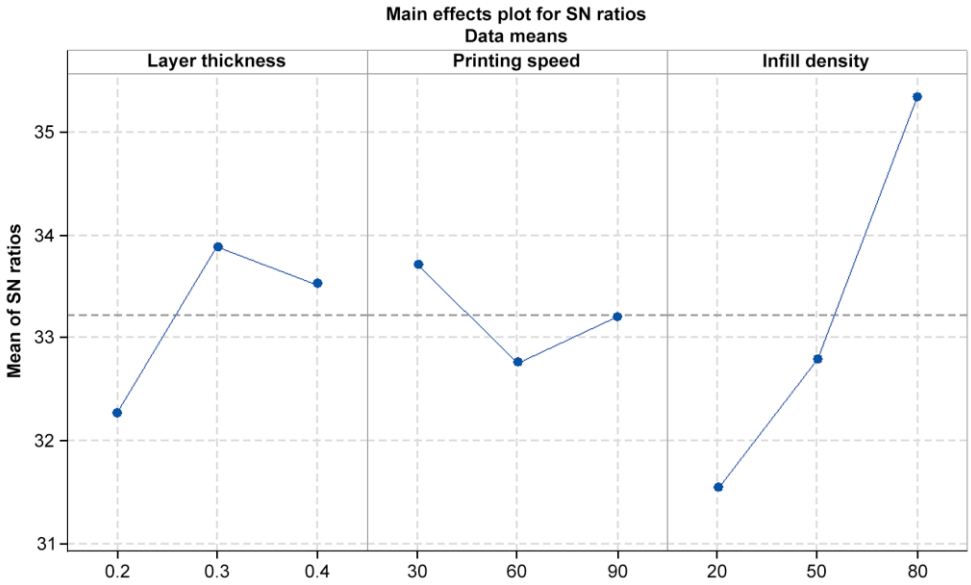

Fig 14 . Main effect plots of signal-to-noise ratios for compressive strengths

Table 12. Optimum parameter settings for the compressive test

Layer thickness (mm)	Printing speed (mm/s)	Infill density (%)
0.3	30	80

The compressive strength can be enhanced by increasing the layer thickness and infill density while reducing the printing speedHigher infill density produces a denser internal structure with improved reinforcing, which usually increases the compressive strength. On the other hand, increasing the printing speed could improve the output but would sacrifice compressive strength. Together with previous research [18], these findings confirm that infill density largely contributes to the compressive strength of the PLA–carbon-fiber-printed samples. Nevertheless, balancing the speed and quality is pivotal for preserving strong material properties. Slower printing speeds allow precise material deposition, strong bonding, and enhanced fiber alignment, leading to products with superior compressive strength. By methodically modifying these parameters and evaluating the resultant compressive strength, we can determine the ideal combination of layer thickness, infill density, and printing speed that improves the compressive strength of 3D-printed PLA–carbon fiber.

4.2.1. Analysis of the printing parameters

The correlations and interactions among layer thickness, infill density, and printing speed were statistically examined using the Taguchi method, akin to the tensile test. This analysis will identify the ideal levels of process parameters to maximize compressive strength. The investigation verifies that raising the infill density typically improves the compressive strength. Increasing the infill density from 20% to 80% enhanced the compressive strength from 37.82 to 63.19 MPa, dependent upon layer thickness and printing speed (Table 8). This phenomenon is due to the more durable, less porous structure created at higher infill densities, which can withstand substantial compressive load. [26]. The favorable correlation between compressive strength and infill percentage is attributable to the diminished amount of air voids and enhanced density, both of which mitigate potential deformation [10].

The microstructures of samples produced with infill densities of 20% and 80% exhibit significant changes (Figure 15a); an infill density of 20% yielded a component with many voids and gaps between the printed layers and within the infill structure, which can potentially concentrate stress and introduce susceptible points prone to failure under applied loads. These unfilled void spaces can also compromise the interlayer adhesion, weakening the interlayer bonds and consequently reducing the overall structural integrity and mechanical characteristics of the printed part. Therefore, reducing the infill density will lower the compressive strength performance from of parts manufactured with higher infill densities. When the infill density reached 80% (Figure 15b), the sample became more solid and was compacted with reinforced carbon fiber separated by minimal gaps. Owing to the heightened density, the sample showed high resistance to applied loads, and its compressive strength was maximized. The reasons for this behavior are discussed in subsection 3.1.2. Prior research has demonstrated the

correlation between infill density and compressive strength. As infill density increases, a larger volume of material fills the spaces within the structure, hence improving load distribution and enhancing the overall compressive strength of the printed component. Further research has demonstrated that reducing infill density leads to structures with many voids, weakening the integrity of the overall structure and reducing its compressive strength [5]. On the contrary, increased infill densities result in a strong internal structure that improves the compressive strength of PLA–carbon-fiber–printed objects.

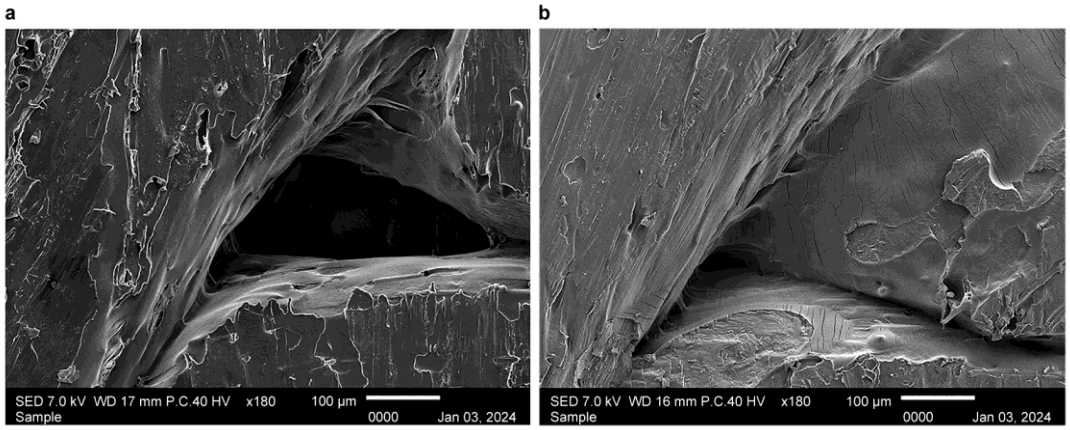

Fig 15 . Microstructural comparison of samples with a) 20% and b) 80% infill density (scale bar = 100 µm) in compressive strength experiment.

In typical cases, reducing the layer thickness of the PLA–carbon-fiber prints also enhances the compressive strength because thin layering strengthens the bonding between layers [2] and hence enhances the uniformity of the structure. Conversely, thicker layering can increase the size of the gaps between layers, potentially introducing weak spots that reduce the overall compressive strength. Like the tensile strength, the compressive strength is further affected by the alignment of the carbon fibers in the PLA–carbon-fiber composites, which themselves influence the orientation and bonding of layers. The current experiment, contrary to known assumptions and prior investigations, demonstrated an increase in compressive strength at layer thicknesses of 0.2 and 0.3 mm, followed by a decrease at a thickness of 0.4 mm. The observed compressive strengths were 51.63, 63.19, and 61.08 MPa for layer thicknesses of 0.2, 0.3, and 0.4 mm, respectively. The variance in compressive strength between samples with layer thicknesses of 0.2 and 0.3 mm may be ascribed to the unique features of the PLA–carbon-fiber composite material. Increasing the layer thickness may aid in the alignment and distribution of carbon fibers within the layers, thereby enhancing load-bearing capabilities and improving overall strength [16]. Increasing the layer thickness further enhances compressive strength by minimizing the number of interfaces, which may lead to a reduction in weak spots or structural discontinuities. At a layer thickness of 0.4 mm, the compressive strength began to decline, indicating that this layer thickness is suboptimal for the printing of PLA–carbon fiber.

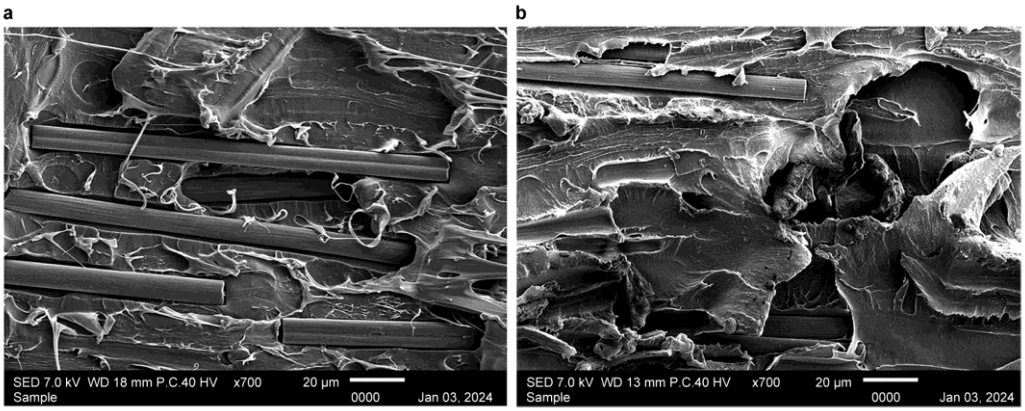

Fig. 16. Microstructural comparison of samples fabricated at printing speeds of a) 30 and b) 90 mm/s (scale bar = 100 µm) in compressive strength experiment.

Referring to Table 4, the compressive strength exhibits no consistent trend with respect to printing speed. Sample 5 had the highest compressive strength of 63.19 MPa, characterized by a layer thickness of 0.3 mm, an infill density of 80%, and a printing speed of 60 mm/s. The second- and third-highest performers were samples

7 (printing speed = 30 mm/s; average compressive strength = 61.08 MPa) and sample 3 (printing speed = 90 mm/s; average compressive strength = 51.63 MPa), respectively. Figure 16 compares the microstructures of the samples fabricated at printing speeds of 30 and 90 mm/s. It appears that reducing the printing speed improves the interlayer bonding by promoting fusion of the adjacent layers during the melting process. Slower deposition and melting of the material fosters robust bonding, as evidenced in the microstructure of experiment Run 5 (Figure 16a). A slower printing speed also ensures a gradual and compact material deposition that minimizes the internal void spaces, thus enhancing the structural integrity and showing an increase in the overall compressive strength of the printed items. In contrast to this finding, the tensile strength improved at higher printing speeds. Previous research has proven that the tensile and compressive strengths of 3D-printed objects do not significantly depend on printing speed. For instance, an ANOVA analysis confirmed that compressive strength is statistically unaffected by printing speed [3]. Relative fiber content greatly affects the tensile mechanical properties of continuous carbon-fiber-reinforced composites; printing temperature and speed have far less effect [8]. While the continuous carbon-fiber phase impacts the tensile mechanical characteristics, the latter two factors mostly affect the fiber-matrix bonding interface of a continuous carbon-fiber-reinforced 3D-printed composite. Printing speed has little effect on the compressive strength of PLA–carbon fibre.

5. CONCLUSIONS

The main aim of this work was to improve the tensile and compressive strengths of PLA–carbon fiber by optimizing the 3D printing parameters through FDM and the Taguchi method. The principal parameters of 3D printing are layer thickness, infill density, and print speed.. The tensile strength of the printed PLA–carbon-fiber significantly depended on both layer thickness and infill density, whereas the compressive strength depended almost entirely on infill density. The following conclusions confirm the fulfillment of the study objectives:
Tensile strength was best at 0.4 mm layer thickness, 80% infill density, and 90 mm/s print speed.
The compressive strength was best at 0.3 mm layer thickness, 80% infill density, and 30 mm/s print speed.
Infill density increased the tensile and compressive strengths of 3D-printed PLA–carbon-fiber samples, but printing speed did not affect mechanical properties.
Microstructural measurements showed that reducing infill density increases voids and air gaps, reducing printed sample tensile and compressive strengths.
This investigation enriches our understanding of 3D printing with PLA–carbon fiber, a composite material with prospective applications across diverse fields requiring robustness and stiffness. Users and manufacturers in the 3D printing realm can enhance the quality and efficacy of their products by judiciously selecting the appropriate printing parameters. This study also underscores the efficacy of the Taguchi technique in optimizing 3D printing procedures.
The study on PLA-carbon fiber composites' tensile and compressive strengths has been optimized, but some limitations need to be addressed through future research. It should explore additional parameters like extrusion temperature, nozzle diameter, and raster orientation, and explore alternative materials like nylon-carbon fiber or PETG-carbon fiber. Long-term durability studies and optimization of functional properties like flexibility, impact resistance, and thermal stability are also needed. Integrating advanced simulation techniques like finite element analysis could provide predictive insights into 3D-printed composites' mechanical behavior. This could lead to improved performance and wider adoption of PLA-carbon fiber composites in high-performance industries.

Author contributions: Conceptualization, design of the study, supervision, review and editing, funding acquisition, Nor Aiman Sukindar; conceptualization, supervision, validation, Mohamad Talhah Al Hafiz Mohd Khata; methodology, resources, project administration, Ahmad Shah Hizam Md Yasir, Shafie Kamaruddin; investigation, data curation, Muhamad Izzat Izzuddin Saharuddin, Ahmad Azlan Ab Aziz, Wan Luqman Hakim Wan A Hamid, Muhammad Mukhtar Noor Awalludin; validation and visualization, Yang Chuan Choong; writing, original draft preparation, Mohamad Talhah Al Hafiz Mohd Khata, Muhamad Izzat Izzuddin Saharuddin; writing, review and editing, Nor Aiman Sukindar. All authors have read and agreed to the published version of the manuscript.
Funding source: This publication was financially supported by Rabdan Academy, 65, Al Inshirah, Al Sa'adah, Abu Dhabi.
Conflicts of interest: There is no conflict of interest.
Acknowledgment: The authors would like to express their sincere appreciation to the School of Design, Product Design, Universiti Teknologi Brunei, and the Advanced Manufacturing and Technology Research Unit (AMTech), Manufacturing and Materials Engineering, International Islamic University Malaysia, for providing the necessary facilities and support throughout the course of this research.

REFERENCES

1. Ahmed, W., Siraj, S., Al-Marzouqi, A. H. (2020). *3D printing PLA waste to produce ceramic-based particulate reinforced composite using abundant silica-sand: Mechanical properties characterization*. Polymers, 12, 1–19. https://doi.org/10.3390/polym12112579
2. Dou, H., Cheng, Y., Ye, W., Zhang, D., Li, J., Miao, Z., Rudykh, S. (2020). *Effect of process parameters on tensile mechanical properties of 3D printing continuous carbon fiber-reinforced PLA composites*. Materials (Basel)*, 13*. https://doi.org/10.3390/ma13173850
3. Maqsood, N., Rimašauskas, M. (2021). *Characterization of carbon fiber reinforced PLA composites manufactured by fused deposition modeling*. Composites Part C: Open Access, 4. https://doi.org/10.1016/j.jcomc.2021.100112
4. Dave, H. K., Rajpurohit, S. R., Patadiya, N. H., Dave, S. J., Sharma, K. S., Thambad, S. S., Srinivasn, V. P., Sheth, K. V. (2019). *Compressive strength of PLA-based scaffolds: Effect of layer height, infill density, and printing speed*. International Journal of Modern Manufacturing Technology, 11, 1–14.
5. Rouf, S., Raina, A., Haq, M. I. U., Naveed, N., Jeganmohan, S., Kichloo, A. F. (2022). *3D printed parts and mechanical properties: Influencing parameters, sustainability aspects, global market scenario, challenges, and applications*. Advances in Industrial Engineering and Polymer Research, 5, 143–158. https://doi.org/10.1016/j.aiepr.2022.02.001
6. Saleh, M., Anwar, S., Al-Ahmari, A. M., Alfaify, A. (2022). *Compression performance and failure analysis of 3D-printed carbon fiber/PLA composite TPMS lattice structures*. Polymers, 14. https://doi.org/10.3390/polym14214595
7. Kamaal, M., Anas, M., Rastogi, H., Bhardwaj, N., Rahaman, A. (2021). *Effect of FDM process parameters on mechanical properties of 3D-printed carbon fibre–PLA composite.* Progress in Additive Manufacturing, 6, 63–69. https://doi.org/10.1007/s40964-020-00145-3
8. Ajay Kumar, M. A., Khan, M. S., Mishra, S. B. (2020). *Effect of fused deposition machine parameters on tensile strength of printed carbon fiber reinforced PLA thermoplastics*. Materials Today: Proceedings, 27, 1505–1510. https://doi.org/10.1016/j.matpr.2020.03.033
9. Jatti, V. S., Sapre, M. S., Jatti, A. V., Khedkar, N. K., Jatti, V. S. (2022). *Mechanical properties of 3D-printed components using fused deposition modeling: Optimization using the desirability approach and machine learning regressor.* Applied System Innovation, 5. https://doi.org/10.3390/asi5060112
10. Wickramasinghe, S., Do, T., Tran, P. (2020). *FDM-based 3D printing of polymer and associated composite: A review on mechanical properties, defects, and treatments*. Polymers, 12, 1–42. https://doi.org/10.3390/polym12071529
11. Ansari, A. A., Kamil, M. (2021). *Effect of print speed and extrusion temperature on properties of 3D printed PLA using fused deposition modeling process*. Materials Today: Proceedings, 45, 5462–5468. https://doi.org/10.1016/j.matpr.2021.02.137
12. Czyżewski, P., Marciniak, D., Nowinka, B., Borowiak, M., Bieliński, M. (2022). *Influence of extruder's nozzle diameter on the improvement of functional properties of 3D-printed PLA products.* Polymers, 14, 356. https://doi.org/10.3390/polym14020356
13. Doshi, M., Mahale, A., Kumar Singh, S. K., Deshmukh, S. (2022). *Printing parameters and materials affecting mechanical properties of FDM-3D printed parts: Perspective and prospects*. Materials Today: Proceedings, 50, 2269–2275. https://doi.org/10.1016/j.matpr.2021.10.003
14. Pavan, M. V., Balamurugan, K., Balamurugan, P. (2020). *Compressive test fractured surface analysis on PLA-Cu composite filament printed at different FDM conditions.* IOP Conference Series: Materials Science and Engineering, 988. https://doi.org/10.1088/1757-899X/988/1/012019
15. Vălean, C., Marșavina, L., Mărghitaș, M., Linul, E., Razavi, N., Berto, F. (2020*). Effect of manufacturing parameters on tensile properties of FDM printed specimens*. Procedia Structural Integrity, 26, 313–320. https://doi.org/10.1016/j.prostr.2020.06.040
16. Lee, D., Wu, G. Y. (2020). *Parameters affecting the mechanical properties of three-dimensional (3D) printed carbon fiber-reinforced polylactide composites*. Polymers, 12, 1–11. https://doi.org/10.3390/polym12112456
17. Li, Y., Lou, Y. (2020). *Tensile and bending strength improvements in PEEK parts using fused deposition modelling 3D printing considering multi-factor coupling*. Polymers, 12, 1–14. https://doi.org/10.3390/polym12112497
18. Liu, G., Zhang, X., Chen, X., He, Y., Cheng, L., Huo, M., Yin, J., Hao, F., Chen, S., Wang, P., Yi, S., Wan, L., Mao, Z., Chen, Z., Wang, X., Cao, Z., Lu, J. (2021). *Additive manufacturing of structural materials.* Materials Science and Engineering R Reports, 145, 100596. https://doi.org/10.1016/j.mser.2020.100596

19.Heidari-Rarani, M., Rafiee-Afarani, M., Zahedi, A. M. (2019). *Mechanical characterization of FDM 3D printing of continuous carbon fiber reinforced PLA composites*. Composites Part B: Engineering, 175, 107147. https://doi.org/10.1016/j.compositesb.2019.107147
20.Kargar, E., Ghasemi-Ghalebahman, A. (2023). *Experimental investigation on fatigue life and tensile strength of carbon fiber-reinforced PLA composites based on fused deposition modeling*. Scientific Reports, 13, 18194. https://doi.org/10.1038/s41598-023-45046-x
21.El Magri, A., Vaudreuil, S. (2021). *Optimizing the mechanical properties of 3D-printed PLA-graphene composite using response surface methodology*. Archives of Materials Science and Engineering, 112, 13–22. https://doi.org/10.5604/01.3001.0015.5928
22.Ganesh Iyer, S. S. G., Keles, O. (2022). *Effect of raster angle on mechanical properties of 3D printed short carbon fiber reinforced acrylonitrile butadiene styrene*. Composites Communications, 32, 101163. https://doi.org/10.1016/j.coco.2022.101163
23.Liu, Z., Lei, Q., Xing, S. (2019). *Mechanical characteristics of wood, ceramic, metal and carbon fiber-based PLA composites fabricated by FDM.* Journal of Materials Research and Technology, 8, 3741–3751. https://doi.org/10.1016/j.jmrt.2019.06.034
24. Ogaili, A. A. F., Basem, A., Kadhim, M. S., Al-Sharify, Z. T., Jaber, A. A., Njim, E. K., Al-Haddad, L. A., Hamzah, M. N., Al-Ameen, E. S. (2024). *The effect of chopped carbon fibers on the mechanical properties and fracture toughness of 3D-printed PLA parts: An experimental and simulation study*. Journal of Composites Science, 8(7), 273. https://doi.org/10.3390/jcs8070273
25. Maqsood, N., Rimašauskas, M. (2021). *Delamination observation occurred during the flexural bending in additively manufactured PLA-short carbon fiber filament reinforced with continuous carbon fiber composite*. Results in Engineering, 11*,* 100246. https://doi.org/10.1016/j.rineng.2021.100246
26. Anand Kumar, S., Shivraj Narayan, Y. (2019). *Tensile testing and evaluation of 3D-printed PLA specimens as per ASTM D638 type IV standard ASTM D638*. In U. Chandrasekhar, L. J. Yang, & S. Gowthaman (Eds.), Innovative Design, Analysis and Development Practices in Aerospace and Automotive Engineering (I-DAD 2018*)* (pp. 79–95). Lecture Notes in Mechanical Engineering, Springer, New York. https://doi.org/10.1007/978-981-13-2718-6_9
27. Jatti, V. S., Sapre, M. S., Jatti, A. V., Khedkar, N. K., Jatti, V. S. (2022). *Mechanical properties of 3D-printed components using fused deposition modeling: Optimization using the desirability approach and machine learning regressor*. Applied System Innovation, 5*,* 112. https://doi.org/10.3390/asi5060112

Received: March 12th, 2025 / Accepted: October 14th, 2025 / Paper available online: December 20th, 2025